Andrey G. Egorov
Arthur A. Salamatin

Kazan Federal University, Department of Aerohydromechanics, Kazan, Russia.

Bidisperse Shrinking Core Model for Supercritical Fluid Extraction

The broken-and-intact-cell model is conventionally used for interpretation of overall extraction curves (OECs) observed in supercritical fluid extraction (SFE) of ground oilseeds. Another possibility, considered here, assumes that the packed beds of the ground material always contain a significant amount of very small particles, i.e., dust, which control the initial extraction rates. The bidisperse representation of particle ensembles allows accurate description of OECs on the basis of the modified shrinking core model. A simple asymptotic solution has been derived for bidisperse granulometric distributions under typical SFE conditions. Special microscopic observations have been performed to reveal and examine the dust fraction in ground seed substrates.

Keywords: Bidisperse granulometric distribution, Polydisperse packed bed, Shrinking core model, Supercritical fluid extraction

Received: October 26, 2014; *revised:* December 25, 2014; *accepted:* April 20, 2015

DOI: 10.1002/ceat.201400627

1 Introduction

Supercritical fluid extraction (SFE) is a novel process more appropriate for extracting natural products from plant material than traditional methods. It is environmentally friendly, provides selective extraction, and employs nonflammable and nontoxic solvents, usually CO_2, without any solvent residues in the final product [1]. In view of these advantages, it is important to scale up this technique for industrial applications. SFE has been increasingly studied during recent decades by various scientific groups both experimentally [2–7] and theoretically, applying mathematical models [5–21] to identify internal mechanisms which control the extraction process. The review in [22] also demonstrates the importance of various supercritical fluids applications, in particular of SFE of oils from plant material.

The principal information on SFE kinetics is conventionally deduced from the overall extraction curve (OEC) whose characteristic shape divides the extraction process into two periods: (i) the initial solubility-limited stage I at a constant (maximum) extraction rate and (2) the subsequent diffusion-controlled stage II with extremely low extraction rates [2–6, 8–18].

Two-stage experiments can be generally described in terms of free and tied oil. It is assumed that the former is generated as a result of oilseed size reduction step, i.e., grinding, crushing, flaking etc. This kind of oil is extracted during stage I. The tied oil is the residual substance which is recovered during stage II at relatively low rates controlled by undestroyed inner plant barriers like membranes, cell walls etc. To reduce net-product costs, it is important to increase the amount of free oil, i.e., to prolong stage I duration.

One of the common ways to describe the stage of free oil extraction is the "broken-and-intact-cells" (BIC) model [10–12] which assumes that cell membranes are the only significant resistance for solute diffusion through the plant matrix and that a developed superficial layer of cells with destroyed membranes (broken cells) exists on the surface of all ground seed particles [10–12]. Hence, the oil extraction from broken cells is limited solely by solubility, and these cells are depleted throughout the stage I of extraction. Stage II, on the other hand, is characterized by very slow extraction from inner cells with intact membranes (intact cells). The BIC model generally agrees with OEC data. Yet, broken cells on the particle surface may be only one of possible receptacles of the free oil and deduced amounts of such cells so far have not been verified in experiments [20].

Here, another physical possibility is considered, namely, an alternative interpretation of free oil, which complements the idea of broken cells in the framework of the so-called shrinking core (SC) model [13–18]. The SC description is also widely used in the SFE theory and basically assumes that the permeability through the cell membranes prevails over the diffusion rates along the cell walls. As a consequence, throughout the extraction process, a sharp transition boundary divides a particle into two zones, i.e., the inner oil-filled core which shrinks during the extraction and the outer transport region of depleted cells. The SC model is also capable to account for the polydispersity of packed beds.

Our direct microscopic observations and laboratory measurements of particle size distributions, presented in the first part of the paper, confirm that not only broken cells are formed

Correspondence: Arthur A. Salamatin (arthouse131@rambler.ru), Kazan Federal University, Department of Aerohydromechanics, Kremlyovskaya Str. 18, Kazan, 420008, Russia.

in the course of the grinding process, but also a great number of very small particles (dust) with large specific surface area (SSA) and short diffusion paths are generated. Thus, the dust fraction, along with broken cells, is predominantly extracted during stage I, whereas the main ensemble of the bigger particles of relatively small SSA is depleted at stage II.

Mathematically, such a physical picture presumes further development of polydisperse SC theory, in particular for bimodal packed beds [15–17], as described in the second part of the paper. The constructed generalized SC model predicts the two-stage character of OECs and closely follows a short-term transition between stages I and II. The model was validated on a variety of SFE experiments with pumpkin [2], apricot [4], sunflower [5], and grape [6] seeds in our earlier publications [16, 17]. A simple asymptotic expansion has been also deduced for typical SFE conditions in case of bimodal granulometric distribution of the substrate.

2 Experimental

2.1 Material

Dried pumpkin seeds were bought at a local market. The shells of the seeds were separated manually. The deshelled grains were ground by means of a coffee grinder. The obtained ground pumpkin substrate was separated into several particle size fractions by sieving. Finally, three batches of yellowish and fatty particles with size ranges (corresponding to sieve meshes) (1) 400–630 μm, (2) 800–1000 μm, and (3) 1000–1250 μm were prepared for microscopic observations, exhaustive Soxhlet extraction, and particle size distribution measurements described further in this section. It should be noted that no SFE experiments were performed, and the ground material was used only for investigation of the packed-bed composition.

2.2 Microscopy

Produced fractions were observed through the light microscope MBS-10. The video camera DCM-800 with 8 Megapixel resolution of 3264×2448 was employed to take photographs.

2.3 Particle Size Distribution Measurements

Particle size distributions were determined on a laser diffraction particle size analyzer Mastersizer 2000 produced by Malvern with the particle-size resolution from 0.1 to 2000 μm; distilled water served as a measurement medium.

To reliably estimate the volume fractions of smaller and bigger particles, each of the selected batches was investigated in the analyzer in three different states: (1) non-extracted sample treated by ultrasound (10 s, 40 W), (2) exhaustively extracted sample without additional treatment, and (3) exhaustively extracted sample treated by ultrasound (10 s, 40 W). The exhaustive extraction was performed by a Soxhlet apparatus using hexane as a solvent at atmospheric pressure. The ultrasound treatment was performed when particles were placed into the analyzer with distilled water, just before size-distribution measurement.

3 Results and Discussion

3.1 Microscopic Observations

It has already been acknowledged [21] that the packed-bed structure may significantly affect the extraction process. With this in mind, special microscopic observations of the three ground-seed batches were conducted to study their composition. Figs. 1 a–c convincingly demonstrate that a lot of tiny particles much smaller in size than the sieve-mesh dimensions do exist in the ground material.

Another peculiarity revealed by Figs. 1 a and 1 b is that these "dust" particles can adhere to the surface of bigger particles or

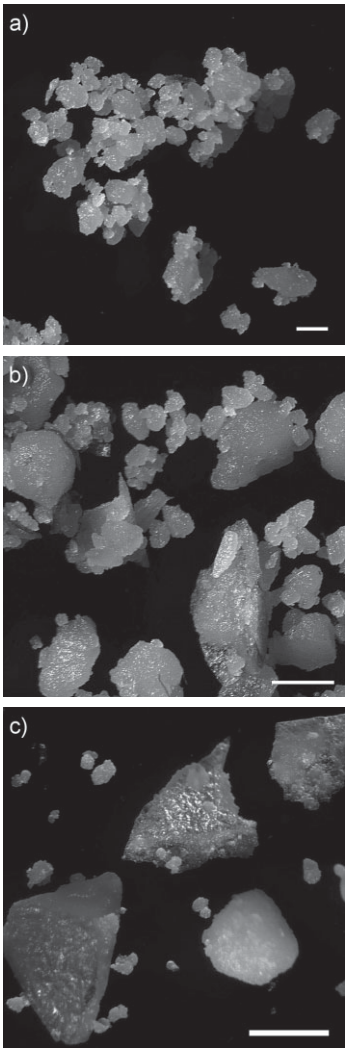

Figure 1. Enlarged images of non-extracted particle fractions with characteristic size: (a) 400–630 μm, (b) 800–1000 μm, and (c) 1000–1250 μm. Scale bars are (a) 400 μm, (b) 800 μm, and (c) 1000 μm.

stick to each other and form aggregates. This agglomeration may be caused by adhesive and/or electrostatic forces. Importantly, a shaking comparable with that of the sieving procedure does not break the aggregates; particles stuck together just reorder or jump to other agglomerates. Thus, the dust fraction, distributed over bigger particles and/or joined in compact groups, cannot be directly distinguished by the particle size and remains "inconspicuous" for sieving analysis. The same features of the ground substrate could be supposed in many other SFE experiments considered in publications.

However, for the bigger-size fractions (compare Figs. 1 a and 1 b with Fig. 1 c) an essentially less amount of dust particles was detected. Sometimes another sort of particles could be observed; they were like snowballs built up of compacted dust. Due to high porosity, such particles might be extracted in the same way as dust. But because of their rare occasions, the volume fraction of these snowball particles is assumed to be negligible.

Nevertheless, it is important to realize that dust may exist in ground material in different forms, adhering to surface of bigger particles, sticking up in agglomerates of several particles, or even joining in big snowball clusters. The dust fraction cannot be effectively discerned by sieving and discriminated by size, it may be present in any fraction of bigger particles. Dust structure and extraction from dust need a closer and more accurate investigation for deeper understanding of the SFE process.

Different fractions of ground particles were also microscopically observed after complete extraction in hexane. They became white after extraction, and a considerable amount of dust with less than 100 μm in diameter was visually detected in each fraction, even in case of 1000–1250 μm particles.

3.2 Particle Distribution Measurements for Individual Fractions

To estimate the dust volume, particle size distributions were measured in different fractions by laser diffraction methods. Logarithmic scales allow a better resolution of specific compositional features for both smaller and bigger particles. The particle volume distribution function $G^{1)}$ of $\lg a$ is introduced as:

$$G(\lg a) = \int_{-\infty}^{\lg a} g(\xi)\,\mathrm{d}\xi \equiv F(a) \tag{1}$$

Hereinafter, $F(a)$ is a particle volume distribution function determined with particle radius a. The density g of the distribution function G is related with the density f of the F-distribution as:

$$f(a) = \frac{g(\lg a)}{a \ln 10}, \quad F(a) = \int_0^a f(\xi)\,\mathrm{d}\xi \tag{2}$$

and the partial volume fraction of particles with size from a to $a+\mathrm{d}a$ is $\mathrm{d}G = g\,\mathrm{d}(\lg a) = \mathrm{d}F = f\,\mathrm{d}a$.

The samples of non-extracted ground material were examined first. Since, in accordance with microscopic observations, ground particles could stick to each other, the ultrasound treatment was intended to break agglomerates and separate particles. The results obtained for particle fractions of different size are presented in Figs. 2 a–c by dashed lines. In all cases, volume fractions of smaller particles with diameter less than 100 μm are found in the range of 55–65 %. However, these ratios could be distorted, i.e., overestimated, by the presence of "false dust" particles which are small solute drops released from the plant material during the experimental procedures. For this reason, exhaustively extracted plant material was also investigated, and the size-distribution measurements were performed with and without ultrasound treatment. It was found that ultrasound treatment did not change much the extracted batch structure. In both cases, the obtained size distributions did not differ significantly, and the average curves are plotted in Figs. 2 a–c by solid lines. Although the measured volume fractions of dust particles in exhaustively extracted plant material appear to be less prominent and fall in the range of 30–45 %, a significant dust component should be envisaged in packed beds, at least of ground oilseeds in SFE modeling and data interpretation. At the same time, it becomes obvious that a certain amount of oil was released from plant material in our experiments, and laser diffraction measurements should be performed with extracted plant material to obtain more adequate results.

A characteristic feature of all size distributions depicted by solid curves in Fig. 2 is that they show two distinct maximums, one in the range of dust particles and another in the field of the sieved particle-size fraction. This observation is the main reason to develop a generalized polydisperse SC model and, in particular, to derive its limiting case for bimodal packed beds as discussed in the following section.

The particle size distributions measured in extracted samples can be used to calculate not only the relative dust-particle volume, but also estimate the total amount of free oil stored in broken cells on the surface of ordinary ground particles as well as in the dust particles. With this in mind, it is assumed that the diameter of dust particles is less than 100 μm, while the thickness of the surface layer of broken cells δ_{BC} is ~48 μm, being on the order of the mean cell diameter. The free-oil volume fractions α, deduced in this exercise, for the three sieved batches are plotted in Fig. 3 by circles. The estimated α-values fall in the range of 60–70 % and are practically the same as those for the apparent dust volumes measured in the non-extracted ground material. The dust-volume fractions previously determined in the exhaustively extracted material are about 30–45 %. Hence, the volumes of dust particles and broken cells are commensurable, and most of the broken cells released their oil content in the form of the "false dust" particles into distilled water when the particle size distributions in the non-extracted batches were measured.

Analogous results, also shown in the Fig. 3 by square markers, were inferred [17] from other available experiments [2] with pumpkin seeds. A certain discrepancy between these two data sets for the smaller-size fractions, namely, 400–630 μm and 250–600 μm [2], may well be due to the difference in the lower-size sieves used in experiments, i.e., 400 μm and 250 μm, respectively, with the smaller-size fraction from [2] containing more dust. As for other two fractions of bigger particles, the free-oil volume estimates are in good agreement with earlier results for pumpkin seeds [2, 16, 17].

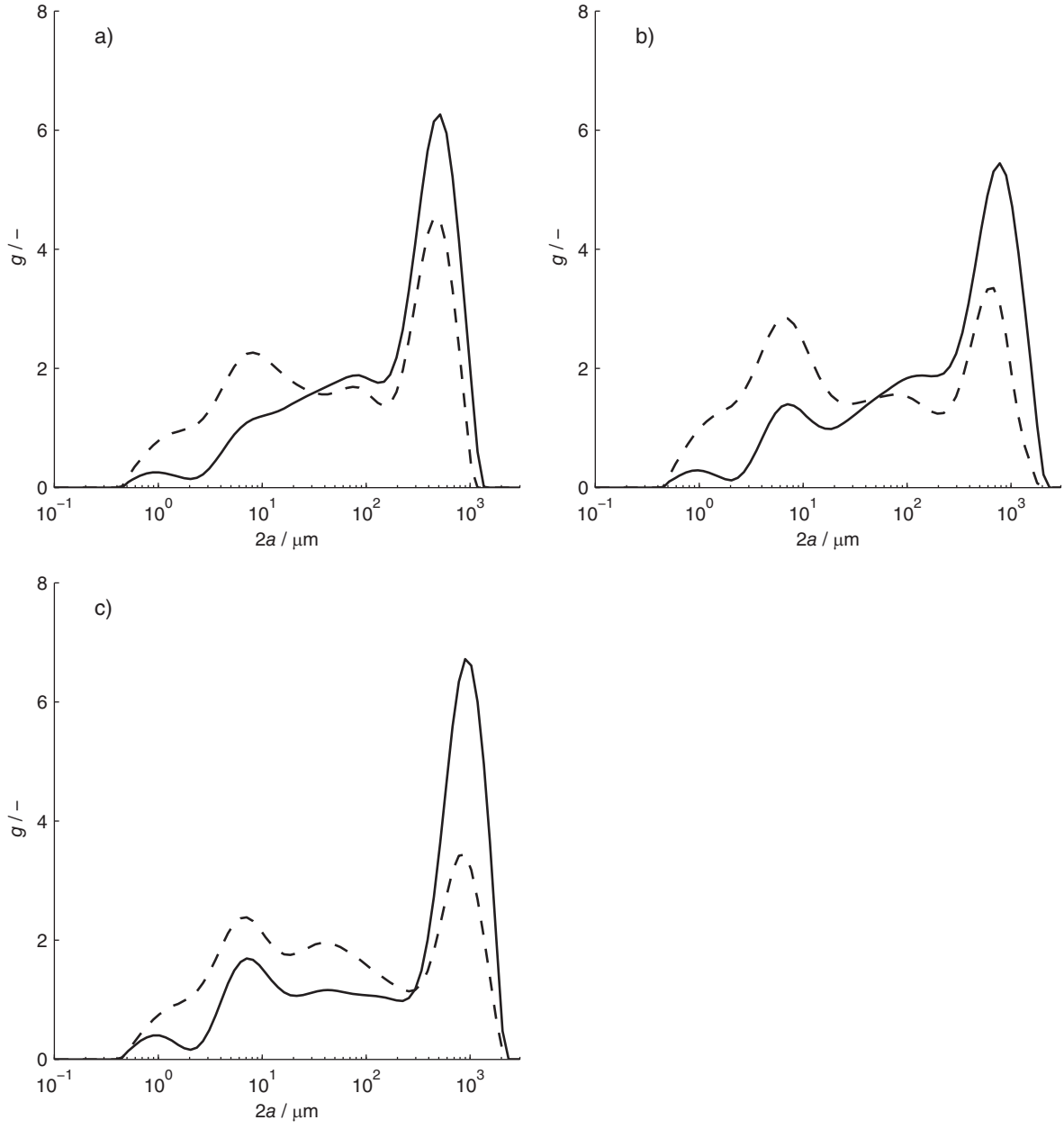

Figure 2. Particle distributions g of (a) 400–630 μm, (b) 800–1000 μm, and (c) 1000–1250 μm fractions. Solid line: extracted particles, dashed line: non-extracted particles.

4 Mathematical Model

4.1 General SFE Model Formulation

In the SFE process, the solvent flows at a constant flow rate through a vessel loaded with the packed bed of ground plant material. The solvent soaks ground particles and dissolves the solute which diffuses through cell walls and intercellular space to the particle's surface. Further, the solvent transports the solute to the outlet from the vessel where the solute is separated form the solvent by depressurization [1, 17].

Plant material size reduction, a common pretreatment procedure in SFE technology, results, as discussed above, in high polydispersity of the initial substrate, even in particular fractions of ground particles sieved in a narrow mesh-size range. Accordingly, a general SC model for the extraction process should be formulated so as to take into account the nontrivial particle size distribution in packed beds of SFE vessels.

Usually, two different limiting types of particle shape approximations are considered in theory: plain (ground leaves) and spherical (isometric crushed seeds). The particle dimension a designates in these cases the half-thickness or radius,

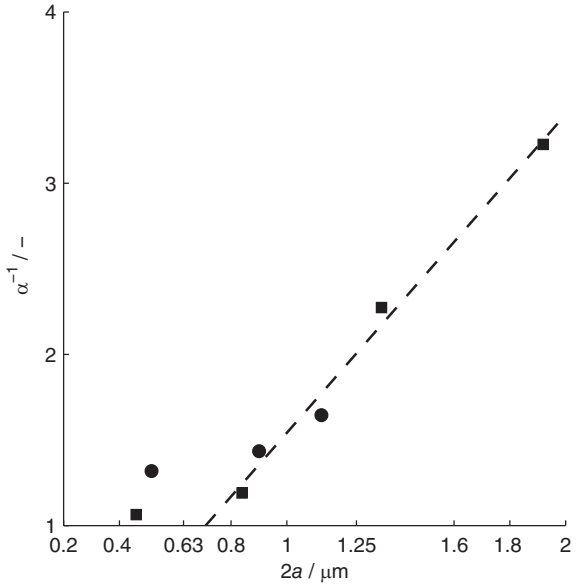

Figure 3. Inverse free oil fraction plotted versus mean particle size of different fractional batches. Square markers correspond to [2], circles to our measurements.

respectively. Here, the following denotations are also introduced: t is the time, z is the spatial coordinate, varying along the flow from 0 to the vessel height H, r is the axial or radial coordinate inside particles of plain or spherical geometry, e means the porosity of the packed bed, v is the solvent flow rate, D is the apparent diffusion coefficient of oil in ground particles, and $c(t, z)$ represents the solute concentration in the liquid phase.

The conventional shrinking core approach in SFE modeling is based [13, 14] on the principal assumption that a sharp concentration boundary is formed and moves inside each particle. This implies essentially low diffusion rates through transport intercell channels in comparison with the cell membrane permeability. As a result, the inner core, $0 \le r \le R$, of non-extracted oil is separated by the narrow diffusive front from the outer depleted transport zone, $R \le r \le a$. The core radius R shrinks, starting from the particle size a and tending to 0 with the extraction progress. Thus, the SC model assumes that the solute diffusion in ground particles solely controls the SFE process, and extraction time scales of particles are inversely proportional to their individual surface areas. As a consequence, a detailed sophisticated description of polydisperse packs becomes a crucial step of SFE model development and application.

General SC master equations of oil mass balance in particles and solute flow can be written in terms of functions $c(t, z)$ and $R(t, z, a)$ according to [13–15, 18]:

$$\theta_0 \frac{\partial R}{\partial t} = -q\left(\frac{a}{R}\right)^{n-1}, \quad q(t,z,a) = \frac{D}{a-R}\left(\frac{a}{R}\right)^{(1-n)/2}(\theta_* - c) \tag{3}$$

$$e\frac{\partial c}{\partial t} + v\frac{\partial c}{\partial z} - D_{ax}\frac{\partial^2 c}{\partial z^2} = q_S = (1-e)\int_0^\infty q(t,z,a)\frac{A(a)}{V(a)}f(a)\mathrm{d}a \tag{4}$$

Here, θ_0 is the initial solute density in the plant material, a ratio of initial mass of oil in a particle to its volume; θ_* denotes the solute solubility in the solvent phase; D_{ax} is the axial dispersion coefficient of apparent convective diffusion; A and V are the respective total surface area and total volume of a-size particles ($A/V = n/a$), and n is the particle shape factor with $n = 1, 3$ for plain and spherical geometry, respectively.

Further, typical scales of the principal characteristics designated hereinafter by subscript sc are introduced:

$$c_{sc} = \theta_*; \quad z_{sc} = H; \quad t_{sc} = \frac{\theta_0}{\theta_*}\frac{H(1-e)}{v}; \quad a_{sc}^2 = 2nD\frac{H(1-e)}{v} \tag{5}$$

and respective dimensionless variables x, ζ, τ, and ξ as

$$c = xc_{sc};\ z = \zeta z_{sc};\ t = \tau t_{sc};\ a = \xi a_{sc} \tag{6}$$

Based on previous estimates [18] for conventional conditions of vegetable oil extraction from seeds with high oil content, e.g., sunflower seed, rapeseed, etc., further the mass transfer in the fluid phase in quasi-stationary convective approximation [9, 12] is described and axial dispersion [8, 9, 11, 12, 14] is neglected. In particular, these simplifications were shown [18] to be valid in case of oilseeds with high initial oil density θ_0 and low oil solubility θ_* in the solute, i.e., for $\theta_0 >> \theta_*$, at high superficial velocities ($v > 10^{-5}\,\mathrm{m\,s^{-1}}$) common for the SFE process. The latter peculiarity also implies that the external oil-mass transfer coefficient from particle surface to solvent flow tends to infinity, as originally assumed in Eqs. (3). As a result, with the use of scales (5) and in terms of normalized characteristics (6), after integration with respect to time, the basic oil-mass conservation Eqs. (3) and (4) take the following simplified dimensionless form:

$$\varphi_n(s) = \min\left\{1; \frac{\tau - y}{\xi^2}\right\}, \quad 0 \le \varphi_n = \int_0^s \frac{\mathrm{d}\omega}{\lambda_n(\omega)} \le 1 \tag{7}$$

$$\frac{\partial y}{\partial \zeta} = \int_0^\infty s\left(\frac{\tau - y}{\xi^2}\right) f(\xi)\,\mathrm{d}\xi \tag{8}$$

Here, the volume fraction $s(\tau, \zeta, \xi)$ of oil extracted from a particle of size ξ, $0 \le s \le 1$, and the mass fraction $y(\tau, \zeta)$ of oil, extracted at time τ from the packed bed within the interval $[0, \zeta]$, $0 \le y \le \zeta$, are introduced as:

$$s = 1 - (R/a)^n \tag{9}$$

$$y(\tau, \zeta) = \int_0^\tau x(\omega, \zeta)\mathrm{d}\omega \tag{10}$$

The cumulative diffusion coefficient $\lambda_n(s)$ in Eq. (7) depends on the particle shape as follows:

$$\lambda_3 = \frac{0.5(1-s)^{1/3}}{1-(1-s)^{1/3}}, \qquad \lambda_1 = \frac{1}{2s} \tag{11}$$

Eqs. (7) and (8) should be completed by the boundary condition:

$$y(\tau,0) = 0 \tag{12}$$

which means that the pure solvent is pumped through the inlet cross section of the vessel.

By definition, the dependence $\varphi_n(s)$ is a monotonic function of s for both spherical and plain particles, $0 \le s \le 1$, and Eq. (7) determines s implicitly to be substituted into Eq. (8). Consequently, the system of simultaneous Eqs. (7), (8), and (12) can be classified as a Cauchy problem with respect to y of ζ with parameter τ.

The modified polydisperse SC model (7), (8), and (12) can be solved [17] analytically with respect to the overall extraction curve $Y(\tau) = y(\tau, 1)$. This solution predicts the full depletion time t_+ of the packed bed as:

$$t_+ = \frac{\theta_0}{\theta_*}\left(\frac{H(1-e)}{v} + \frac{a_{\max}^2}{2nD}\right) \tag{13}$$

where $a_{\max}$ is the maximum particle size in the pack.

Constrained [16, 17] by various SFE data, the apparent diffusion coefficient was inferred on the order of $D \sim 10^{-13}\,\mathrm{m^2 s^{-1}}$. Thus, the second term in the latter relation for t_+ prevails over the first one, at least in laboratory experiments when H is of the order of 10 cm.

4.2 Monodisperse Packed Beds

A monodisperse packed bed is the simplest possible approximation of particle size distribution. It is commonly used in SFE modeling especially when a single fraction of ground particles is selected for extraction after sieving and the packed bed is assumed to be homogeneous [19]. In this case, the modified SC model (7), (8), and (12) depends only on one tuning parameter, namely, the diffusion coefficient D, i.e., in dimensionless representation, on the normalized particle size ξ scaled in accordance with Eqs. (5) and (6).

However, the monodisperse model fails to match OECs when a series of experiments with different particle size fractions of the same ground material is considered (see Fig. 4) under the assumption that parameters D and θ_0 are independent of particle size and solute concentration. For instance, this approximation, being in agreement with the extraction curves for fractions of smaller particles (squares in Fig. 4), does not predict the observed two-staged extraction for bigger particles. Although indirectly, this fact also points to the inner inhomogeneity of the sieved particle fractions.

4.3 Bimodal Packed Beds

The above-mentioned problem of OECs interpretation can be solved if a so-called bimodal packed-bed approximation is assumed. It is a particular case of polydisperse packed beds that accounts for the existence of two prominent modes in particle volume distributions, e.g., as observed in our experiments.

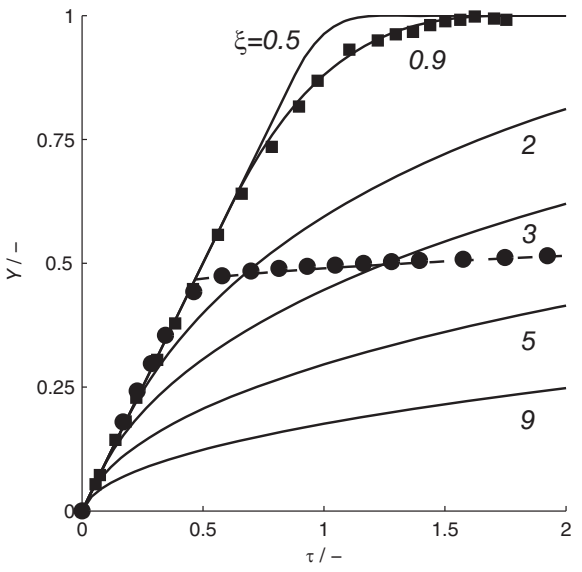

Figure 4. Experimental and modeled OECs for different particle sizes of monodisperse fractions. Solid lines: modeled OECs for monodisperse approximation, corresponding numbers denote the dimensionless particle size ξ. Squares: experimental results for extraction of tomato seeds [13], circles: for pumpkin seeds [2], dashed line: asymptotic solution.

Thus, in the framework of the bimodal packed-bed approximation, the apparent dust fraction, i.e., dust particles together with the broken cells, represents free-oil containers. In this scenario, the extraction from the dust fraction with large SSA dominates during the initial stage I. Stage II of extraction starts when the dust is fully depleted, and only particles of the second (bigger size) mode remain in the process.

Mathematically, in terms of the polydisperse SC model, the bimodality corresponds to a special form of the density function $f(\xi)$:

$$f(\xi) = \alpha f_1(\xi) + (1-\alpha) f_2(\xi) \tag{14}$$

where α is the volume fraction of dust, while f_1 and f_2 are the unimodal density functions which describe the size distribution of dust particles with typical dimensions of $\sim 100\,\mu\mathrm{m}$ or less and that of the ordinary particles of $\sim 200\,\mu\mathrm{m}$ in size and bigger, respectively.

A limiting case of the bimodal packed beds is the bidisperse pack, i.e., a homogeneous mixture of two particle fractions of fixed radii ξ_1 and ξ_2 with corresponding volume ratios α and $(1–\alpha)$. This packed bed is characterized by a stepwise distribution function F with the corresponding density function f in Eq. (14) as a combination of two Dirac functions, $f_i = \delta(\xi–\xi_i)$, $i = 1,2$.

Accordingly, Eq. (8) takes the form [5, 19]:

$$\frac{\partial y}{\partial \zeta} = \alpha s\left(\frac{\tau - y}{\xi_1^2}\right) + (1-\alpha) s\left(\frac{\tau - y}{\xi_2^2}\right) \tag{15}$$

The general applicability of monodisperse approximation for modeling the SFE process in the fraction of ordinary, big par-

ticles, described here in terms of f_2, was demonstrated in simulations [19] performed for Gaussian particle size distributions with different dispersions in the framework of the Reverchon-Marrone model [20]. In case of the SC concept, this approach was also discussed and validated on available experimental data in [16, 17].

The simplified bidisperse pack model was shown [16] to be sufficient for many laboratory-scale experiments [2, 4–6] which are relatively short with respect to the full depletion time when the bigger (ordinary) particle shapes do not noticeably affect the extraction process.

An asymptotic expansion for OEC can be derived [17] on the order of ε^2 error in this case, when only SSA of big particles, i.e., ξ_0^{-1}, controls the extraction process:

$$Y = \alpha + \frac{2}{3}\varepsilon\left(\tau^{3/2} - (\tau-\alpha)^{3/2}\right) + O(\varepsilon^2), \quad \varepsilon = \sqrt{n}\frac{1-\alpha}{\xi_0\alpha} \tag{16}$$

$$\tau_- = \alpha + \frac{2}{3}\varepsilon\alpha^{3/2} + O(\varepsilon^2), \quad \xi_0^{-1} = \int_0^\infty \frac{f_2(\xi)}{\xi}\,\mathrm{d}\xi \tag{17}$$

Here, τ_- is the duration of stage I.

Relationship (16) is valid for normalized extraction times $\tau_- < \tau << \xi_0^2$ with τ_- given by expression (17); obviously, in accordance with the normalization procedure (5) and (6), in dimensionless form, $Y(\tau) = \tau$ for $\tau < \tau_-$.

Various available experiments with representative monodisperse (single fraction) [2, 4] and polydisperse [5, 6] beds were used in [16, 17] to validate and constrain the model (7), (8), and (12) in bidisperse approximation. The simulations performed in [16, 17] also demonstrated general applicability and high accuracy of asymptotic expansion (17) and (18). For instance, here we illustrate the convergence of the asymptotic solution and close agreement of the developed bidisperse model with the SFE data on the basis of Salgin and Korkmaz's experiments [2]. The corresponding best-fit model parameters inferred in [17] are gathered in Tab. 1. The simulated (solid lines) and asymptotic (dashed lines) yield curves are compared with each other and with the measurements [2] in Figs. 4 and 5.

Table 1. SC model parameters for bidisperse approximation of a packed bed composed of pumpkin seeds [2]. $D = 1.2 \times 10^{-12}\ \mathrm{m^2 s^{-1}}$, $\theta_0 = 212\ \mathrm{kg\,m^{-3}}$; $\theta_* = 7.7\ \mathrm{kg\,m^{-3}}$.

Curve number	1	2	3	4
Mean radius of big fraction particles a_2 [mm]	0.23	0.42	0.67	0.96
Dust fraction α	0.94	0.84	0.44	0.31

5 Conclusions

Direct microscopic observations show that, along with the broken cells assumed by the BIC model, a significant amount of tiny crushed particles (dust) exist in ground plant material in different forms, i.e., adhering to the surface of bigger particles, sticking up in agglomerates, or even joining in big snowball clusters. The dust fraction cannot be effectively discerned by sieving and discriminated by size; it may be present in any sieved fraction of ordinary particles. Both broken cells and dust represent the free oil receptacles and have been introduced in the polydisperse (bimodal) SC model as a separate (apparent) dust fraction which allowed for matching OECs with high accuracy.

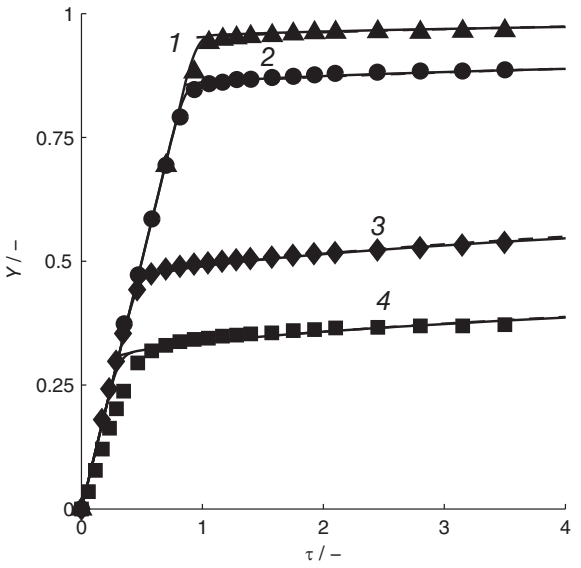

Figure 5. Model adaptation for SFE of pumpkin seeds [2]. Solid lines: modeled OECs, markers: experiments; curve numbers refer to the Tab. 1. Dashed lines which coincide with solid curves: asymptotic solution.

Both BIC and polydisperse SC models can be applied, at least in principle, to simulate the process of oil extraction from inner intact cells of ground particles at stage II and to closely reproduce OECs recorded in relatively short-term laboratory experiments. In most cases, the obtained SFE data is not sufficient to distinguish between particular intra-particle mass transfer mechanisms. Further specially designed experimental studies are needed to provide a detailed realistic picture of oil distribution in non-extracted and partly extracted particles [23] as well as to give reliable estimates for volume fractions of broken cells.

The necessity to use polydisperse SFE models also requires adequate measurements of particle size distribution. It is clear that the sieving analysis, as a basic method for particle size quantification, does not capture all the structural details of ground plant material and, e.g., does not allow correct estimation of its SSA. From this point of view, particle size distributions obtained by the laser diffraction method seem to be more reliable and consistent with the direct microscopic observations. Laser diffraction may also provide valuable information about dust fractions in each particular case of plant material and way of particles reduction, e.g., flaking, grinding, chopping etc.

Acknowledgment

The authors like to thank G. E. Bekmukhamedov and A. Z. Kurbangaleeva of the Butlerov Institute of Chemistry (Kazan Federal University) for particle size distribution measurements and useful scientific discussions. We are also grateful to I. F. Safin of the Department of Criminal Process and Criminalistics (Kazan Federal University) for providing the access to microscopes. Our special thanks should be addressed to R. S. Khaziev and A. S. Makarova of the Kazan State Medical University for the preparation of extracted plant material as well as to P. V. Zelenihin and A. I. Kolpakov of the Institute of Fundamental Medicine and Biology (Kazan Federal University) for their help in microscopic observations. The authors are grateful to anonymous referees for valuable comments and stimulating suggestions which helped to revise and improve the paper.

The work was supported by the Russian Foundation for Basic Research and the Republic of Tatarstan, grant No. 15-41-02542 r_povolzhe_a.

The authors have declared no conflict of interest.

Symbols used

A	[m^2]	total surface area of particles with size a
a	[m]	half-thickness for plain particles and radius of spheres
a_{max}	[m]	maximum particle size in the bed
c	[$kg\,m^{-3}$]	solute concentration in the liquid phase
D	[m^2s^{-1}]	effective diffusion coefficient of oil in ground particles
D_{ax}	[m^2s^{-1}]	axial dispersion coefficient
e	[–]	porosity of the packed bed
F	[–]	particle size distribution function with respect to a
f	[m^{-1}]	density of distribution function F
G	[–]	particle size distribution function with respect to lg a
g	[–]	density of distribution function G
H	[m]	vessel height
n	[–]	particle shape factor; $n = 1, 3$ for plain and spherical particles, resp.
R	[m]	size of inner core which shrinks with the extraction progress
r	[m]	spatial coordinate inside particles
s	[–]	volume fraction of extracted oil
t	[s]	time
t_+	[s]	time of packed-bed full depletion
V	[m^3]	total volume of particles with size a;
v	[$m\,s^{-1}$]	fluid superficial (filtration) velocity
x	[–]	dimensionless solute concentration in the liquid phase ($x = c/c_{sc}$)
Y	[–]	OEC, volume fraction of oil extracted from a packed bed
y	[–]	fraction of oil, extracted from a part of packed bed [0;z]
z	[m]	spatial coordinate, varying from 0 to H, from its inlet to outlet

Greek letters

α	[–]	volume fraction of dust
δ_{BC}	[m]	height of superficial layer of broken cells
ζ	[–]	dimensionless spatial coordinate, varying from 0 to 1, from its inlet to outlet ($\zeta = z/z_{sc}$)
θ_0	[$kg\,m^{-3}$]	initial solute density, a ratio of initial mass of oil in the particle to its volume
θ_*	[$kg\,m^{-3}$]	solute solubility in the solvent phase
λ_n	[–]	cumulative diffusion coefficient which depends on particle shape
ξ	[–]	dimensionless particle size ($\xi = a/a_{sc}$)
τ	[–]	dimensionless time ($\tau = t/t_{sc}$)
τ_-	[s]	dimensionless duration of stage I of extraction

Subscripts

sc	scale for corresponding variable
1	dust fraction
2	fraction of big (ordinary) particles

Abbreviations

OEC	overall extraction curve
SC	shrinking core
BIC	broken-and-intact cell
SFE	supercritical fluid extraction
SSA	specific surface area

References

[1] J. W. King, in *Lipid Biotechnology* (Eds: T. M. Kuo, H. W. Gardner), Marcel Dekker, New York **2002**.

[2] U. Salgin, H. Korkmaz, *J. Supercrit. Fluids* **2011**, *58 (2)*, 239–248. DOI: 10.1016/j.supflu.2011.06.002

[3] C. P. Passos, R. M. Silva, F. A. Da Silva, M. A. Coimbra, C. M. Silva, *J. Supercrit. Fluids.* **2009**, *48 (3)*, 225–229. DOI: 10.1016/j.supflu.2008.11.001

[4] S. G. Ozkal, M. E. Yener, L. Bayindirli, *J. Supercrit. Fluids* **2005**, *35 (2)*, 119–127. DOI: 10.1016/j.supflu.2004.12.011

[5] L. Fiori, *J. Supercrit. Fluids* **2009**, *50 (3)*, 218–224. DOI: 10.1016/j.supflu.2009.06.011

[6] L. Fiori, *J. Supercrit. Fluids* **2007**, *43 (1)*, 43–54. DOI: 10.1016/j.supflu.2007.04.009

[7] Z. Zekovic, S. Filip, S. Vidovic, S. Jokic, S. Svilovic, *Chem. Eng. Technol.* **2014**, *37 (12)*, 2123–2128. DOI: 10.1002/ceat.201400322

[8] E. L. G. Oliveira, A. J. D. Silvestre, C. M. Silva, *Chem. Eng. Res. Des.* **2011**, *89 (7)*, 1104–1117. DOI: 10.1016/j.cherd.2010.10.025

[9] R. N. Patel, S. Bandyopadhyay, A. Ganesh, *Energy Convers. Manage.* **2011**, *52 (1)*, 652–657. DOI: 10.1016/j.enconman.2010.07.043

[10] K. Rochova, H. Sovova, V. Sobolik, K. Allaf, *J. Supercrit. Fluids* **2008**, *44 (2)*, 211–218. DOI: 10.1016/j.supflu.2007.10.007

[11] H. Sovova, *J. Supercrit. Fluids* **2005**, *33 (1)*, 35–52. DOI: 10.1016/j.supflu.2004.03.005

[12] H. Sovova, *Chem. Eng. Sci.* **1994**, *49 (3)*, 409–414. DOI: 10.1016/0009-2509(94)87012-8
[13] B. C. Roy, M. Goto, T. Hirose, O. Navaro, O. Hortacsu, *Jpn. J. Chem. Eng.* **1994**, *27 (6)*, 768–772. DOI: 10.1252/jcej.27.768
[14] M. Goto, B. C. Roy, T. Hirose, *J. Supercrit. Fluids* **1996**, *9 (2)*, 128–133. DOI: 10.1016/S0896-8446(96)90009-1
[15] A. G. Egorov, A. B. Mazo, R. N. Maksudov, *Theor. Found. Chem. Eng.* **2010**, *44 (5)*, 642–650. DOI: 10.1134/S0040579510050027
[16] A. A. Salamatin, A. G. Egorov, R. N. Maksudov, V. A. Alyaev, *Vestnik KNITU / Herald of Kazan National Research Technological University* **2013**, *16 (22)*, 74–77.
[17] A. G. Egorov, A. A. Salamatin, R. N. Maksudov, *Theor. Found. Chem. Eng.* **2014**, *48 (1)*, 43–51. DOI: 10.1134/S0040579514010011
[18] R. N. Maksudov, A. G. Egorov, A. B. Mazo, V. A. Alyaev, I. S. Abdullin, *Sverhkriticheskie Fluidy: Teoriya i Praktika / Supercritical Fluids: Theory and Practice* **2008**, *3 (2)*, 20–32.
[19] L. Fiori, D. Basso, P. Costa, *J. Supercrit. Fluids* **2008**, *47 (2)*, 174–181. DOI: 10.1016/j.supflu.2008.08.003
[20] E. Reverchon, C. Marrone, *J. Supercrit. Fluids* **2001**, *19 (2)*, 161–175. DOI: 10.1016/S0896-8446(00)00093-0
[21] F. Meyer, M. Stamenic, I. Zizovic, R. Eggers, *J. Supercrit. Fluids* **2012**, *72*, 140–149. DOI: 10.1016/j.supflu.2012.08.022
[22] E. Schutz, *Chem. Eng. Technol.* **2007**, *30 (6)*, 685–688. DOI: 10.1002/ceat.200600297
[23] A. Femenia, M. Garcia-Marin, S. Simal, C. Rossello, M. Blasco, *J. Agric. Food Chem.* **2001**, *49*, 5828–5834. DOI: 10.1021/jf010532e

